2013 European Control Conference (ECC)
July 17-19, 2013, Zürich, Switzerland.

Modeling and Analysis of an Atmospheric Driven Atmos Clock with Mechanical Escapement Control

Shreyas Patel, David Moline, and John Wagner, PhD, PE, *Senior Member, IEEE*

***Abstract*—The classic Atmos mantle clock operates on atmospheric differences to power the mechanical bellows and wind the mainspring. A delicate gear train and verge turn a torsional pendulum with minimal frictional losses throughout the system. A pair of hands display the time on a dial in twelve hour increments. In this paper, an Atmos 540 clock has been investigated as it offers vivid insight into a mechanical escapement controller with integrated system components, and a "green" temperature and/or pressure driven power source. The clock design, operation, and mathematical model representing the energy flow through the system will be presented. Representative experimental and analytical results will be introduced and discussed to demonstrate the clock's functionality. Finally, the question of whether this clock meets the definition of a perpetual motion machine will be examined.**

I. Introduction

THE concept of time keeping has existed for many millenniums with the earliest clocks based on natural occurrences. During the 13th century, the monasteries in Europe were agricultural, technical, and spiritual complexes. To synchronize the daily collective prayer times, mechanical weight-driven clocks were introduced to indicate the need to manually ring the bells for prayers [1]. A horology goal since the 18th century has been a perpetual motion clock which does not require winding in any manner. An interesting development in 1928 was the creation of a "living on air" clock by Jean-Leon Reutter (1899-1971), a Neuchatel, Switzerland engineer who graduated from the Zurich Federal Institute of Technology in 1921 as a mechanical engineer. Atmos clock production was principally started by Compagnie Générale de Radio, a French firm in 1929. Jaeger-LeCoultre (Le Sentier, Switzerland), a renowned Swiss watch manufacturer, developed variants of the Atmos clock and began production in 1935 [2]. This clock receives the energy necessary to maintain time by changes in the local atmospheric temperature and pressure. The concept of a perpetual motion machine supports the idea to achieve indefinite output with minimum input; however, the Atmos clock conforms to fundamental thermodynamic laws [3].

Shreyas Patel is with the Mechanical Engineering Department, Clemson University, Clemson, SC 29634 USA (e-mail: smpatel@g.clemson.edu)

David Moline is with the Electrical and Computer Engineering Department, Clemson University, Clemson, SC 29634 USA (e-mail: moline@clemson.edu)

John Wagner is with the Mechanical Engineering Department, Clemson University, Clemson, SC 29634 USA (corresponding author: 864-656-7376, Fax: 864-656-4435,e-mail: jwagner@clemson.edu)

Using a torsion pendulum, which oscillates very slowly about its center of rotation, the Atmos clock requires significantly less energy than a mechanical clock with an ordinary pendulum. The torsional pendulum is suspended by a very fine Elinvar wire. Elinvar, a steel alloy, is often used to make watch springs because of its linear elasticity characteristics over a wide temperature range. Unlike other torsion pendulum clocks which require outside energy sources to wind the mainspring, the Atmos clock is kept wound by the movement of its mechanical bellows. The bellows contain a gas called chloroethane or ethyl chloride, C_2H_5Cl, which is colorless and flammable. It has a boiling temperature of 12.3°C, so at normal room temperature it remains in a vapor condition [4]. As the surrounding temperature changes it causes the expansion or the contraction of this gas, which provides bellows motion. The displacement of the bellows stores energy in the mainspring. The spring unwinding runs the gear train and provides intermittent impulses to operate the torsional pendulum via the clock escapement. The gear train motion and translation of that motion to the pendulum via the escapement, accounts for most of the power losses in the clock mechanism.

A brief literature review of the Atmos clock and horology will be presented. A detailed historical basis of the Atmos clock design and production was written by Lebet in collaboration with Jaeger-LeCoultre [2]. Vacheron *et al.* [5] provided a repair and maintenance guide for the clock. The company literature provides Atmos clock operation, parts, and repair information [6]. In the 1920s, Von Loessl [7] studied the atmospheric influences on clock operations. Moon and Stiefel [8] performed clock escapement experiments to understand nonlinear characteristics such as noise and vibrations. Lepschy *et al.* [9] examined a Ktesibios water clock, verge and foliot clock, and the Huygens pendulum clock to investigate feedback control mechanisms for speed control. Gordon and Giauque [10] studied ethyl chloride properties such as vapor pressure, heat capacity, and heat of fusion. They collected extensive experimental data and established property values for different conditions. Lastly, Callaway [11] and Paradiso and Starner [12] investigated energy harvesting methods for mobile and wireless devices from atmospheric heat, light, and human movements, including the Atmos clock design. The harvesting of energy from atmospheric temperature and pressure changes using strategies such as chloroethane (or similar) charged bellows will gain greater attention.

Fig. 1: Atmos 540 clock investigated in this study circa 1984-1989

This paper explores the functional significance of the Atmos clock components and investigates the energy flow throughout the system. A nonlinear mathematical model of the clock will be derived based on science and engineering concepts. The subsequent computer simulation results will be compared to the experimental results gathered using an Atmos 540 clock as shown in Fig. 1. The remainder of the article is organized as follows. Section II explains the Atmos clock components and their operations. Section III contains the mathematical representation of the clock divided into subsystems. The experimental and numerical results have been placed in Section IV. Section V contains the conclusion and future research scope.

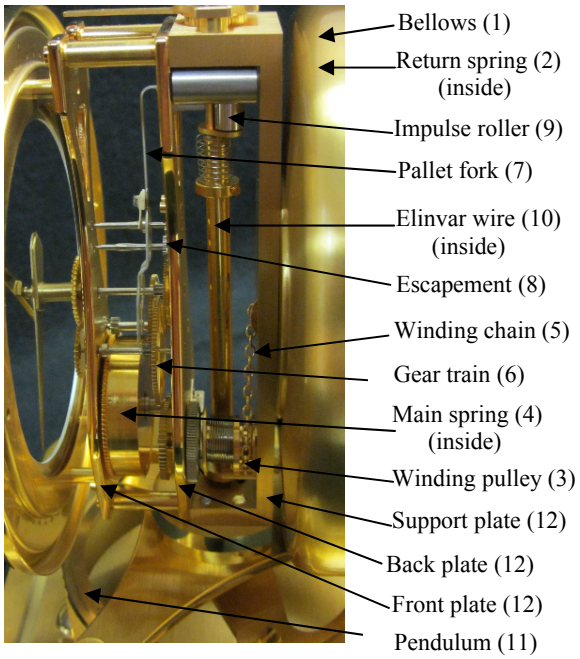

Fig. 2: Labeled components of the Atmos 540 clock [13]

II. Atmos Clock Components and Operation

An overview of the clock's motion works illustrates the mechanical nature of the device. In Fig. 2, the key parts of an Atmos 540 clock are labeled based on company literature [13]. Table I offers a summary of these components.

TABLE I
SUMMARY OF CLOCK COMPONENTS AND DESCRIPTIONS

No.	Component	Description
1	Bellows	Clock power source with ideal gas
2	Return spring	Spring force opposes bellows expansion; returns to nominal
3	Winding pulley	Converts translational motion into rotational motion
4	Main spring	Winds on bellows contraction; maintains position on expansion
5	Winding chain	Chain pulled due to bellows contraction to wind main spring
6	Gear train	Transfers rotational motion from main spring to escape wheel
7	Pallet fork	Accelerates pendulum through impulse roller based on escape wheel interactions
8	Escapement	Converts rotational motion of gear train into pallet fork motion
9	Impulse roller	Transfers impulses from pallet fork to drive Elinvar wire
10	Elinvar wire	Steel alloy wire; hosts pendulum
11	Pendulum	Balance wheel suspended by thin gauge wire
12	Plates	Front, back, and support plates hold components

The bellows is the sole power source for the clock. When the bellows expands and contracts, it displaces a small winding chain connected to a pulley on the mainspring arbor. The pulley is connected to the clock's mainspring so that a one way ratchet only allows spring winding for tension to operate the clock wheels. The wheels power the escapement mechanism and also turn the clock hands. Specifically, the pallet fork causes the Elinvar wire and the torsional pendulum to oscillate back and forth. This pendulum motion stabilizes the escapement motion which allows the clockworks to advance in equal time intervals.

III. Mathematical Model

The mathematical equations which describe the Atmos clock mechanism will be derived using a lumped parameter modeling approach. The energy flow through the clock subsystems [14] will be examined beginning with the atmospheric changes acting on the bellows all the way through to the pendulum motion. Fig. 3 shows the mechanical Atmos clock with the subsystems identified that will be modeled.

A. *Winding Energy Produced by Bellows*

The clock harvests the energy needed to wind the mainspring from the thermodynamic behavior of the constrained fluid within the bellows. The vapor pressure verses temperature phase diagram for chloroethane or ethyl chloride, C_2H_5Cl, in Fig. 4 shows that it's a vapor at room temperature and normal atmospheric pressure. Within the bellows, the fluid may be under sufficient pressure due to the initial charge for both states (liquid and vapor) to exist. Consequently, the gage pressure difference across the bellows follows this curve. In cases where only vapor resides, then the pressure-temperature characteristics will conform to the ideal gas law.

For Atmos clocks, as the ambient air temperature rises, the chloroethane temperature will increase due to conductive heat transfer effects across the bellow's walls. As shown in Fig. 4, a temperature increase results in a larger vapor pressure which drives this power source against the external forces such as the return spring and surrounding atmospheric pressure. The process is repeated in a reverse manner for a decrease in ambient air temperature.

The vapor pressure inside the bellows due to a change in the atmospheric temperature can be obtained using Antoine's equation [15] as

$$\log(p_b) = \left(a - \left(b/(T+c)\right)\right) \tag{1}$$

where p_b is the bellows pressure (bar), T is the temperature, and a, b, and c are ethyl chloride curve fit parameters.

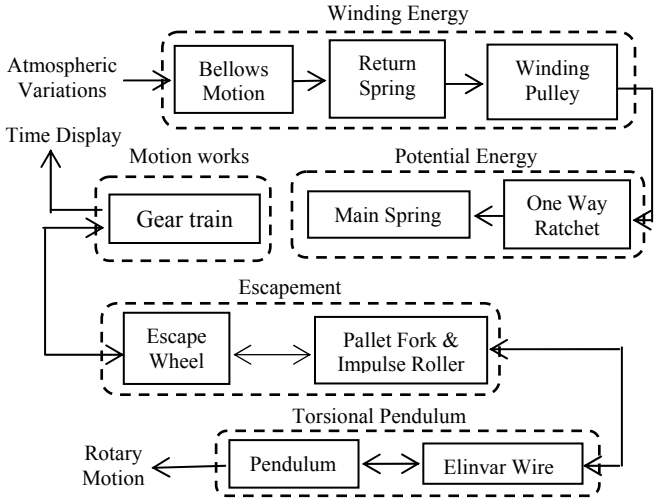

Fig. 3: Interaction of the five mechanical subsystems in the Atmos 540 clock to realize the uniform characterization of time

Once the liquid is converted into a gas (or vapor), the pressure rise inside the bellows can be estimated using the ideal gas law

$$p_b v_b = nRT \tag{2}$$

where v_b is the gas volume in the bellows, n is the number of moles of gas found by dividing the gas mass, m_g, by the molecular mass per mole, M, and R is the ideal gas constant. The term p_b now has units of Pa.

The translational motion of the mechanical bellows is initiated by the expansion of the contained ethyl chloride which produces a driving force, f_b, given as

$$f_b = a_p p_b \tag{3}$$

with a_p denoting the bellows end cap surface area.

The bellows driving force will be opposed by the atmospheric pressure acting on bellows' surface area, the return spring force, f_s, and a spring attached chain force, f_c, which engage the winding pulley and attaches to the one way ratchet as shown in Fig. 5. The equation of motion for the bellows end plate, y, can be written using Newton's law as

$$m_b \ddot{y} = f_b - f_a - f_s - f_c \tag{4}$$

where m_b is the end plate mass.

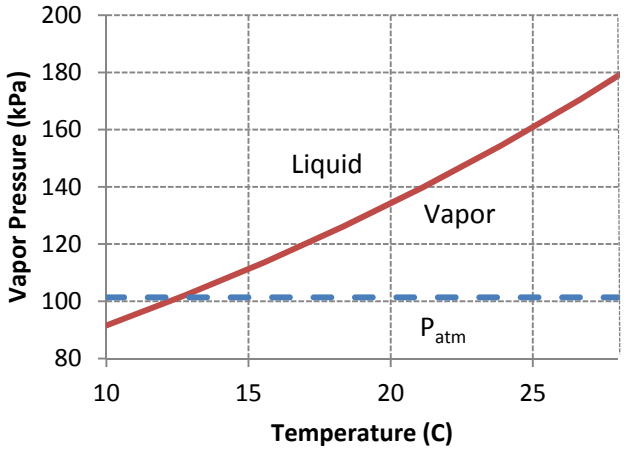

Fig. 4: Vapor pressure versus temperature characteristic for chloroethane or the former name ethyl chloride [12]

The atmospheric force, f_a, acting on the bellows surface area can be expressed as

$$f_a = a_p p_a \tag{5}$$

with p_a representing the local atmospheric pressure.

A stiff return spring, k_{ec}, acts on the end cap to return the bellows to a contracted position when the temperature decreases so that the spring force becomes

$$f_s = k_{ec} y \tag{6}$$

The bellows displacement causes the attached chain to move forward and backward, which rotates the idler pulley and winds the mainspring through the click or ratchet on the contraction stroke. The force exerted by the chain, f_c, can be expressed as

$$f_c = k_c y + f_{click}(\theta_0) \tag{7}$$

where k_c denotes the small spring attached to the end of the chain near the bellow end cap.

The winding pulley is attached to Arbor 0 which also holds the ratchet and main spring. The ratchet is a wheel with saw-shaped teeth that only allows rotation in one direction. A pawl is a pivoted arm that engages the wheel teeth. When the ratchet rotates in one direction, the pawl moves past the ratchet and allows it to rotate. When the ratchet tries to rotate in the other direction, the pawl slips into a tooth on the ratchet wheel preventing motion. For most ratchets, there may be some space between the location of the pawl and the closest tooth of the ratchet. The result is that Arbor 1 may experience a small degree of back spin.

The force exerted by the click, f_{click}, will be a function of Arbor 0 angular displacement, θ_0, such that

$$f_{click}(\theta_0) = \left\{ \begin{array}{c} \frac{1}{r_r}\,\tau_{11};\ \theta_0 > 0 \\ 0\ ;\ \theta_0 \le 0 \end{array} \right\} \quad (8)$$

where $\theta_0 = y/r_p$ with r_p and r_r denoting the winding pulley radius and ratchet wheel radius, respectively. The variable τ_{11} represents the mainspring torque.

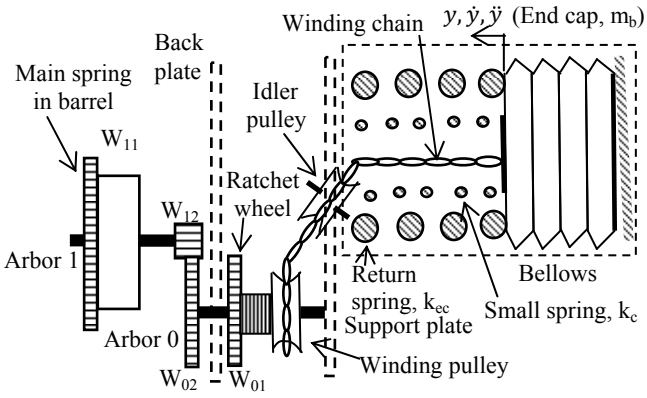

Fig. 5: Transformation of bellows end cap motion into main spring rotational winding for power generation

B. Potential Energy of Mainspring

The mainspring in the Atmos clock is a torsion spring composed of thin gauge coiled steel. The inner end of the mainspring is affixed to Arbor 1 which is wound by the bellows' motion induced chain displacement. The outer end of the spring is attached to the mainspring barrel's wall.

The mainspring is maintained by the ratchet and pawl mechanism which keeps the spring from unwinding in an uncontrolled manner. A wound mainspring stores energy, which is then slowly released to operate the clock mechanism through the escapement. The drive torque, τ_{11}, produced by the mainspring may be expressed as [16]

$$\tau_{11} = \frac{Eb_{ms}t_{ms}^{3}(\theta_1 - \theta_{10})}{12L} \quad (9)$$

where E is the modulus of elasticity for the spring material, b_{ms} is the main spring width, t_{ms} is the main spring thickness, L is the spring length, θ_1 is the angular rotation of Arbor 1, and θ_{10} is the arbor's initial angular displacement.

C. Motion Works

A gear train changes the speed, torque, and/or the direction of rotation for interfaced rotating shafts with wheels. The gear ratio, R_g, between two intermeshed gears is the ratio of their angular velocities, ω, diameter, D, number of teeth, N, and/or torque, τ, so that

$$R_g = \frac{\omega_{in}}{\omega_{out}} = \frac{D_{out}}{D_{in}} = \frac{N_{out}}{N_{in}} = \frac{\tau_{out}}{\tau_{in}} \quad (10)$$

where the subscripts in and out denote the input and output motions. For this application, Fig. 6 offers a representation of the gear train in the timekeeping mechanism with the six arbors supported by the front and back brass plates.

Gears which share the same arbor will have the same angular velocity. The exception to this statement is the hour cannon which rotates around the same axis as the minute gear on Arbor 4. However, the hour cannon receives its input from the gear on Arbor 3. The number of teeth for each wheel and pinion is listed in Table II. The overall gear ratio for the minute hand, R_m, the hour hand, R_h, and the escapement, R_e, can be calculated as

$$R_m = \left(\frac{N_{22}}{N_{11}}\right)\left(\frac{N_{32}}{N_{21}}\right)\left(\frac{N_{42}}{N_{31}}\right) \quad (11)$$

$$R_h = \left(\frac{N_{22}}{N_{11}}\right)\left(\frac{N_{32}}{N_{21}}\right)\left(\frac{N_{43}}{N_{33}}\right) \quad (12)$$

$$R_e = \left(\frac{N_{22}}{N_{11}}\right)\left(\frac{N_{32}}{N_{21}}\right)\left(\frac{N_{42}}{N_{31}}\right)\left(\frac{N_{52}}{N_{41}}\right)\left(\frac{1}{N_{51}}\right) \quad (13)$$

As expected, a 12:1 ratio exists between the minute and hour hands (i.e., minute hand rotates 12 times for one full rotation of the hour hand). Similarly, the 60:1 ratio between the escapement and minute hand reflects the fact that the pendulum period is 60 seconds. If the twin pallets are considered, then the impulse rate is 120 events per hour.

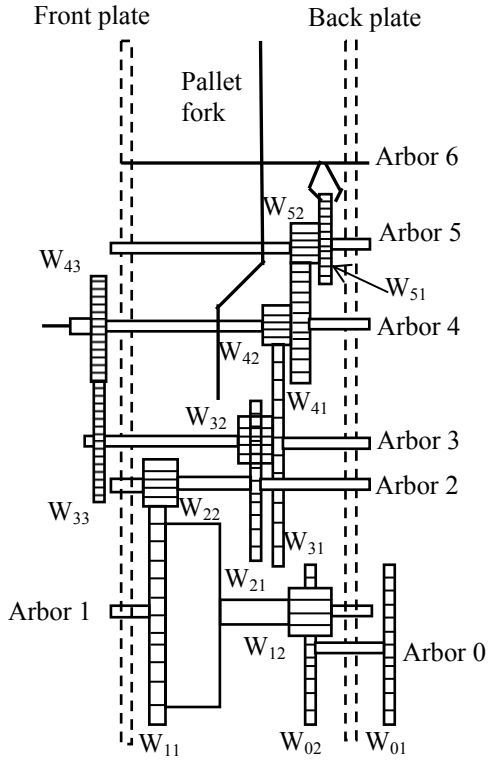

Fig. 6: Atmos 540 motion works with labeled arbors and wheels

D. Escapement

The rotational motion from the gear train is transferred to the pendulum's oscillations by the escapement. The pallet fork keeps the escape wheel from rotating uncontrollably; the twin pallets interact with the escape wheel teeth and transfer the contact force to the impulse roller. The pallet fork and impulse roller interaction may be characterized as a small, 5 seconds in duration, impulse with mechanical shock at the leading edge which occurs every 30 seconds.

The force exerted on the Arbor 6 pallets can be approximately determined (refer to Fig. 7a) as

$$f_{pallet} = f_{tooth}/\tan\theta \quad (14)$$

where f_{pallet} is the force exerted by the pallets, $f_{tooth} = \tau_{51}/r_{51}$ with $\tau_{51} = R_e\tau_{11}$ is the escape wheel tooth generated

force on the pallet jewels, and θ is the angle between the pallet force vector and the normal force, f_n, at the point of contact. The angle between the normal and pallet forces, θ, will vary but can be approximated for now.

TABLE II
SUMMARY OF ATMOS 540 CLOCK MOTION WORKS
(*COMBINED WEIGHT OF ARBOR AND WHEELS)

Arbor	Wheel	Symbol	N	D (mm)	Weight* (gm)
0	1	W_{01}	84	18.90	-
	2	W_{02}	55	18.50	
1	1	W_{11}	103	37.03	16.0
	2	W_{12}	18	6.20	
2	1	W_{21}	87	25.07	2.1
	2	W_{22}	11	4.28	
3	1	W_{31}	87	25.07	2.6
	2	W_{32}	10	3.07	
	3	W_{33}	29	12.40	
4	1	W_{41}	80	18.21	3.6
	2	W_{42}	10	3.09	
	3	W_{43}	40	16.75	
5	1	W_{51}	15	8.95	0.3
	2	W_{52}	20	4.70	

The force transferred to the impulse roller from the pallets, f_{roller}, can be calculated as

$$f_{roller} = \left(\frac{r_{61}}{r_{62}}\right) f_{pallet} \quad (15)$$

where r_{61} is the radius of pallet rotation, and r_{62} denotes the distance from Arbor 6 (point P) center to point Q.

The position vector $\bar{r}_{62}$ from P to Q may be denoted as

$$\bar{r}_{62} = a_1\hat{\imath} + b_1\hat{\jmath} + c_1\hat{k},\ |r_{62}| = \sqrt{a_1^2 + b_1^2 + c_1^2} \quad (16)$$

where a_1, b_1, and c_1 are the x, y, z coordinates of the pallet fork or lever arm.

The roller torque, τ_{roller}, exerted on the pendulum through the impulse roller can be expressed as

$$\tau_{roller} = (r_7 \cos\theta_{iR}) f_{roller} \quad (17)$$

where r_7 is the impulse roller rotation radius and θ_{iR} is the angle of the impulse roller's rotation per Fig. 7b.

The last expression (17) may be rewritten by substituting (14) and (15) so that

$$\tau_{roller} = \frac{r_{61} r_7 \cos\theta}{r_{51} r_{62} \tan\theta_{iR}} \tau_{51} \quad (18)$$

where $\theta_{iR} = \begin{Bmatrix} \theta_p & ; |\theta_p| < 120° \\ 120 sgn(\theta_p) & ; |\theta_p| \geq 120° \end{Bmatrix}$ with θ_p denoting the pendulum's angle of rotation.

E. Torsional Pendulum

The torsional pendulum in the Atmos clock vibrates by rotating clockwise (CW) and counter-clockwise (CCW) about its vertical axis. The impulse roller receives two torque impulses in opposite directions from the crutch at an interval of every 30 seconds. The differential equation of motion for the torsion pendulum becomes

$$J\frac{d^2\theta_p}{dt^2} + B\frac{d\theta_p}{dt} + C\theta_p = \begin{Bmatrix} \tau = +\tau_{roller}\ ; 90^\circ < \theta < 120^\circ \\ \tau = 0; otherwise \\ \tau = -\tau_{roller};\ -90^\circ < \theta < -120^\circ \end{Bmatrix} \quad (19)$$

where $J = \frac{1}{2} m r_{tp}^2$ is the torsional pendulum inertia, B is the damping coefficient, and C is the Elinvar wire stiffness.

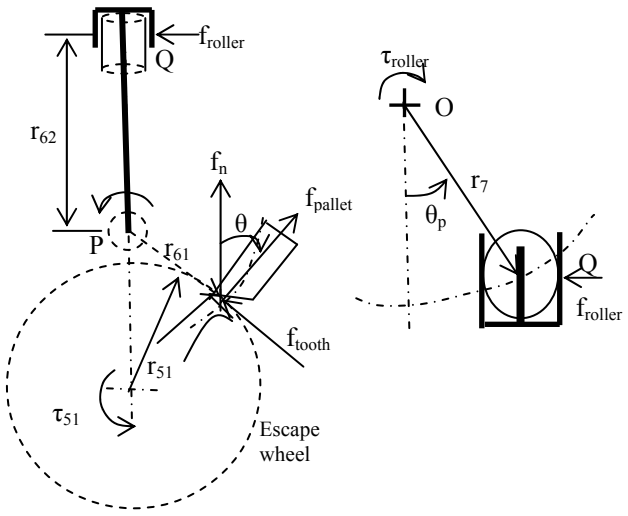

Fig. 7: Escapement and impulse roller geometry (a) front, and (b) top views for two different rotational positions

IV. EXPERIMENTAL AND NUMERICAL RESULTS

A donated Atmos 540 clock served as the basis for the laboratory investigation and accompanying numerical study. In this section, the thermodynamic behavior of the bellows will be examined through prescribed ambient temperature gradients. Next, the attached clock sensors, with accompanying computer based data acquisition system, will be reviewed. Finally, a representative set of experimental and simulation results will be discussed to offer insight into the models and clock operation.

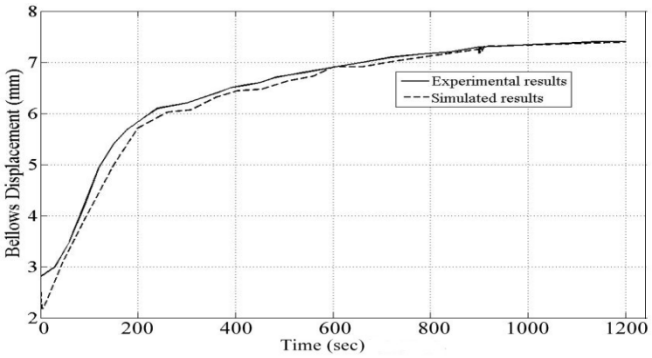

Fig. 8: Experimental and simulated bellows displacement response

A. Bellows Thermodynamic Response

The thermal response of the ethyl chloride gas, sealed inside the bellows, has been experimentally studied by removing the bellows from its canister with return spring, placing it inside a freezer, removing it, and then allowing it to warm to room temperature. The bellows contracted to a minimal size and then gradually expanded as the internal gas warmed through combined conduction and free convective heat transfer. The temperature range for both the experiment and simulation was 272-295 K over a 20 minute time period. No external loading was applied to the bellows;

a thin metal plate was used to improve the vertical position viewing. As shown in Fig. 8, the experimental and simulated results show fairly good agreement.

B. Instrumentation and Data Acquisition

Real time data acquisition has been performed using three attached sensors (refer to Fig. 9) and the LabView software package from National Instruments. A linear output magnetic field (Hall effect) sensor, AD22151, measured the crutch motion. Two high resolution magnetic angular position sensors, APS00B, captured the pendulum and minute hand motions. The sensor outputs were collected and displayed in LabView using a simultaneous sampling multifunction DAQ (NI PCI-6143) kit.

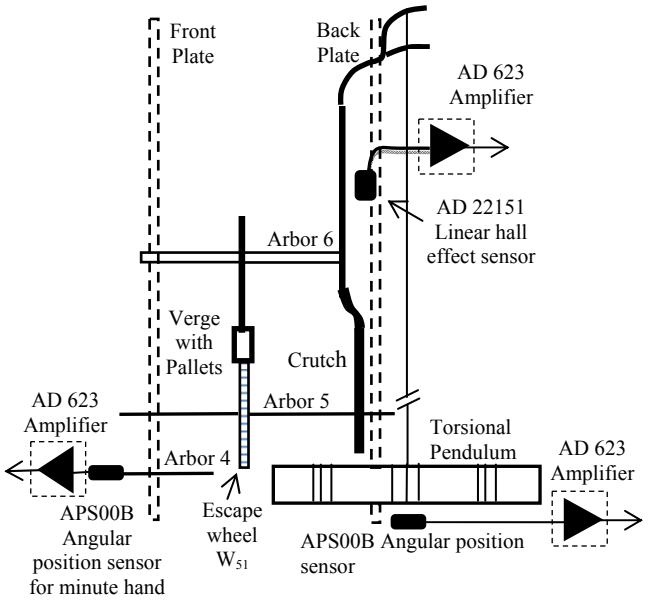

Fig. 9: Side view of clock escapement with attached instrumentation to measure the crutch, pendulum and minute hand motions

C. Comparison of Clockwork and Escapement Motion

The numerical results for the integrated bellows, clockworks, escapement, pendulum, and hands were generated using The Mathworks based Matlab/Simulink models per Fig. 3. The model parameters, listed in Table III, are based on measured system components and physical values obtained from various references.

The experimentally measured minute hand angular motion versus time has been displayed in Fig. 10 per a two minute time interval. Note that the minute hand ticks two times per minute providing approximately 3° of rotation for each clock tick. Further, the transition between angular values was not linear, but features some discontinuities which were dependent on the crutch behavior to be discussed below.

The crutch motion, captured with the high resolution magnetic angular position sensor, versus impulse roller angular motion has been shown in Fig. 11. The crutch remains in a 'hold' position for a significant portion of the time, and moves in one direction for a small span of time every 30 seconds. This event occurs twice per minute in opposite directions. Notice that the recoil of the minute hand (attached to Arbor 4) occurs just as the crutch starts to move. The remainder of the motion profile may be described as a jump of almost equal magnitude at the start of the impulse, the linear motion range, and lastly a large jump (free spin) which happens just before the crutch stops.

TABLE III
SUMMARY OF MODEL PARAMETERS

Symbol	Value	Units	Symbol	Value	Units
a	4.1618	bar	p_a	1	atm
a_p	28.3	cm^2	r_p	4	mm
a_1	28	mm	r_r	9.45	mm
b	1052.82	bar*K	r_{tp}	40	mm
b_{ms}	5.97	mm	r_{51}	4.48	mm
b_1	3.6	mm	r_{61}	2.39	mm
B	15	N*s/mm	r_{62}	31.6	mm
c	-32.078	K	r_7	4.355	mm
c_1	14.2	mm	R	8.314	J/mole*K
C	2	N/mm	R_e	1/42,524	-
E	206,843	MPa	R_h	1/59.06	-
J	400	N/mm^2	R_m	1/708.73	-
k_c	0.1	N/mm	t_{ms}	0.08	mm
k_{ec}	162.79	N/mm	v_b	0.00027	m^3
L	1,100	mm	θ	0.80	rad
m_b	0.2039	kg	θ_p	$\pi/4$	rad
m_g	1.38	g	θ_{10}	0	rad
M	64.514	g/mole	τ_{11}	0.0594	N*mm
n	0.0288	-	τ_{51}	1.4×10^{-6}	N*mm

The crutch provides two torque impulses in opposite directions to the impulse roller which rotates the torsional pendulum. The pendulum motion was measured with an angular position sensor resulting in two rotations per minute as shown in Fig. 12. The simulation results closely follow the experimental data with an approximate 10% difference between them which may be largely attributed to system disturbances and a relatively simplistic escapement model. Overall, the performance of the derived model allows the general operation of the Atmos 540 to be investigated and evaluated against the observed experimental behavior.

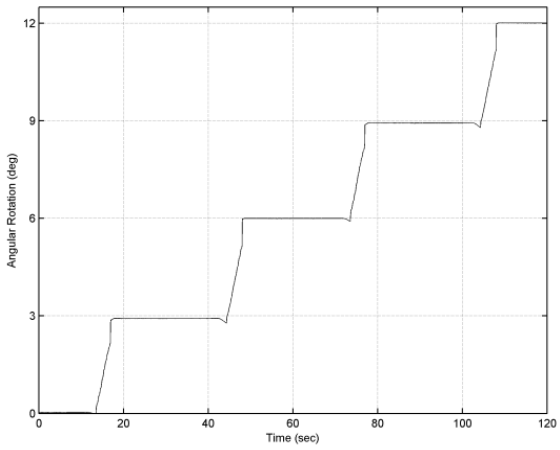

Fig. 10: Experimental minute hand angular motion captured by the angular position sensor for Atmos 540 clock

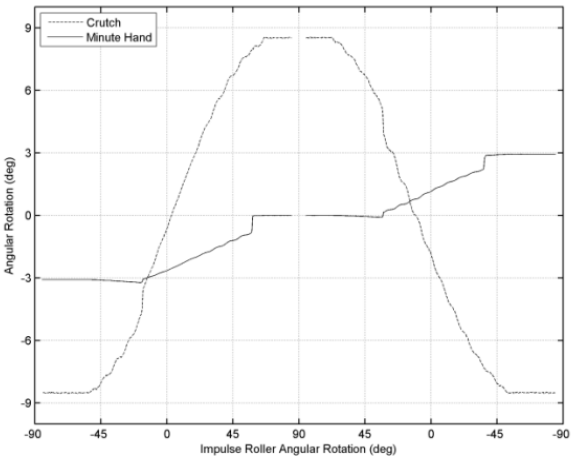

Fig. 11: Experimental crutch and minute hand angular displacement measured over a one minute time period

V. Conclusion

A suite of mathematical models have been developed to describe and analyze the operation of an atmospheric driven Atmos mechanical clock. As reported by Roup and Bernstein [17], the mechanical clock escapement vividly illustrates a feedback regulator to maintain accurate time. System power losses due to friction and uncertainty have been minimized through the use of a delicate escape wheel to pallet fork interface and carefully manufactured gears. Further, the torsional pendulum offers greater efficiency than a common vertical hung pendulum due to reduced operating speed and air resistance. Although the Atmos clock concept is approximately 75 years old, its design remains very creative and timeless. The atmospheric clock provides excellent lessons for capturing mechanical power from an ideal gas to drive a mechanical system which may be labeled as a "green" power source. The Atmos clock cannot be labeled a perpetual motion machine given that it regularly harvests energy from atmospheric temperature and pressure changes to operate the clockworks with little maintenance. Simply put, the Atmos design may be warmly characterized as an innovative thermodynamic machine.

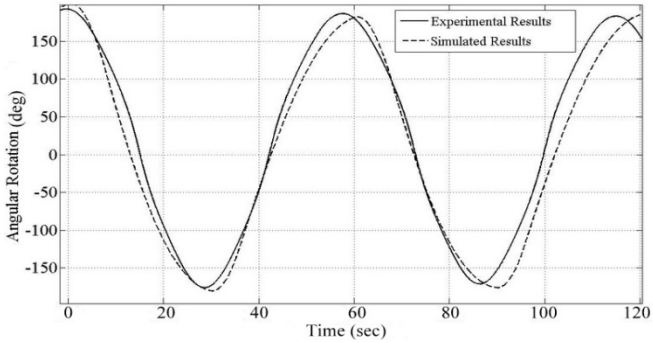

Fig. 12: Torsional pendulum motion experimental and simulated data

Acknowledgments

The authors wish to thank Dr. Errol Ger (Wilmington, DE), Mrs. Helen Bunting (Seneca, SC), and NAWCC Western Carolina Chapter 126 (Asheville, NC) for the donated Atmos Calibre 528-6 and 540 clocks.

References

[1] J. Burke and R. Ornstein, "The Axemaker's Gift", Tarcher/Penguin: New York, NY, 1997.
[2] J. Lebet, "Living on Air: History of the Atmos Clock", Jaeger Le Coultre: Le Sentier, Switzerland, 1997.
[3] G. Wylen and R. Sonntag, "Fundamentals of Classical Thermodynamics", Wiley & Sons: New York, NY, 1978.
[4] E. Martt, "The Atmos Clock Ethyl Chloride as the Bellows Gas", National Association of Watch and Clock Collectors, Horological Science Chapter #161, Horological Science Newsletter, Issue 3, pp. 16, May 1998.
[5] M. Vacheron, M. Constantin, and J. Pierson, "How to Repair Atmos: The Perpetual Motion Clock", Le Coultre Watches, Incorporated, Clockworks Press: Sacramento, CA, 2000.
[6] Jaeger Le Coultre, "Atmos 540 Repair Guide", Jaeger Le Coultre: Le Sentier, Switzerland, April 1993.
[7] F. Von Loessl, "Horloges a Remontage Automatique Par Les Influences Atmospheriques (Clocks with Automatic Winding by Atmospheric Influences*)", Journal Suisse d'Horlogerie*, pp. 45-47, February 1928.
[8] F. C. Moon and P. D. Stiefel, "Coexisting Chaotic and Periodic Dynamics in Clock Escapements", *Journal of Philosophical Transactions of the Royal Society A Mathematical, Physical and Engineering Sciences*, vol. 364, no. 1846, pp. 2539-2564, September 2006.
[9] A. M. Lepschy, G. A. Mian, and U. Viaro, "Feedback Control in Ancient Water and Mechanical Clocks*", IEEE Transactions of Education*, vol. 35, no. 1, pp. 3-10, February 1992.
[10] J. Gordon and W. Giauque, "The Entropy of Ethyl Chloride. Heat Capacity from 13 to 287K. Vapor Pressure. Heats of Fusion and Vaporization", *Journal of the American Chemical Society*, vol. 70, no. 4, pp.1506-1510, April 1948.
[11] E. H. Callaway, Jr., "Wireless Sensor Networks – Architecture and Protocols", Auerbach Publications: Boca Raton, FL, 2004.
[12] J. A. Paradiso and T. Starner "Energy Scavenging for Mobile and Wireless Electronics*", IEEE Journal of Pervasive Computing,* vol. 4, no. 1, pp. 18-27, March 2005.
[13] M. Fritz, "Reverso – The Living Legend", Braus: Berlin, Germany, 1992.
[14] D. Moline, J. Wagner, and E. Volk, "Model of a Mechanical Clock Escapement", *American Journal of Physics,* vol. 80, no. 7, pp. 599-606, July 2012.
[15] National Institute of Standards and Technology, NIST Chemistry Web Book – NIST Standard Reference Database Number 69, (http://webbook.nist.gov/cgi/cbook.cgi?ID=C75003&Units=SI&Mask=1EFF), accessed April 2012.
[16] R. Norton, "Machine Design – An Integrated Approach", Prentice Hall: Upper Saddle River, NJ, 2000.
[17] A. V. Roup and D. S. Bernstein, "Dynamics of the Escapement Mechanism of a Mechanical Clock", proceedings of 38th Conference on Decision & Control, WeP11, Phoenix, AZ, December 1999.